Supporting Information

for

Triplet State of the Semiquinone – Rieske Cluster as an Intermediate of Electronic Bifurcation Catalyzed by Cytochrome bc_1

Marcin Sarewicz, Małgorzata Dutka, Sebastian Pintscher, Artur Osyczka

Simulations of EPR spectra

Low temperature X-band EPR spectra, measured for samples containing antimycin-inhibited cyt bc_1 frozen at different time points, were initially analyzed with *principal component analysis* (PCA). This method revealed presence of two differentially weighted constituents. One of them was recognized as the well-known FeS Rieske cluster spectrum defined by rhombic **g** and **g-strain** tensors, while the second component represented a less anisotropic signal with a new, distinct line at g = 1.94 of unknown origin. The appearance of this new signal can be rationalized on the basis of general magnetic coupling between two closely separated paramagnetic species which in our case are semiquinone at the Q_o site (SQ_o) and the reduced FeS cluster. Indeed, relative arrangement of these two S = ½ centers, inferred from the crystal structure[1] and MD modeling of cytochrome (cyt) bc_1 complex[2], allows for magnetic interaction between the paramagnetic centers. The possible inter-center magnetic coupling can include the dipole - dipole and spin-spin exchange interactions.

To verify which mechanism of interaction responsible for appearance of a new EPR signal is dominant, we performed simulations based on the following spin Hamiltonian, representing the Zeeman interaction of each spin with the external static magnetic field and general bilinear spin-spin interaction:

$$H = \beta \mathbf{B} \cdot \mathbf{g_1} \cdot \mathbf{S_1} + \beta \mathbf{B} \cdot \mathbf{g_2} \cdot \mathbf{S_2} + \mathbf{S_1} \cdot \mathbf{J} \cdot \mathbf{S_2}$$

where $\mathbf{g}_1$ and $\mathbf{g}_2$ refer to magnetic tensors of FeS cluster (with spin $\mathbf{S_1}$) and SQ_o (spin $\mathbf{S_2}$), respectively, **B** – denotes the vector of the external static magnetic field, **J** is the coupling tensor that includes an isotropic (scalar exchange) and anisotropic (exchange and dipolar) terms of magnetic interactions between centers, β - Bohr magneton.

The calculations were carried out in the principal axes system (PAS) of $\mathbf{g_1}$, which was chosen as the reference frame. Within that frame both tensors $\mathbf{g_1}$ (with rhombic symmetry) and $\mathbf{g_2}$ (isotropic) are diagonal, but not necessarily **J**. Neglecting antisymmetric terms of **J,** this tensor can be decomposed into isotropic and traceless, anisotropic parts:

$$J = J_o \cdot I + \begin{pmatrix} J_X & 0 & 0 \\ 0 & J_Y & 0 \\ 0 & 0 & J_Z \end{pmatrix}$$

The expected limiting value of J_o can be estimated based on distance dependence of magnitude of exchange couplings[3]: $|J_0| < 0.5$ cm^{-1}. Assessment of the anisotropic part of **J,** using Moriya equation[4] with appropriate **g**-tensor values gives:

$$|J_i| < \left(\frac{\Delta g}{g}\right)^2 \frac{J}{4}$$

In our case the estimated order of anisotropic terms is negligible as it is about 0.5% J_o. The effect of exchange interaction on the shape of the EPR spectrum of coupled paramagnetic centers depends on relation between the value of J_o and the difference between the resonance frequencies of interacting centers[5]. In our case we have:

$$|J_i| \leq |\Delta g \beta B| \frac{1}{h} \leq |J_o|$$

where: h – Planck constant, B – the resonance magnetic field (~0.33 T or 1.2 T for X -, Q – band, respectively), Δg – the difference between isotropic $g_2 = 2.004$ (SQ_o) and g_{1x}, or g_{1y} or g_{1z} (FeS).

Thus the expected effect of the exchange on EPR spectrum of the coupled centers is that the isolated lines (at g_{1x}, g_{1y}, g_{1z}, g_2) coalesce into signals at positions defined by the arithmetic mean of the sum $\mathbf{g_1} + \mathbf{g_2}$ [5]. Taking the numerical values: $\mathbf{g_1}$ (2.023, 1.89, 1.77) and $\mathbf{g_2}$ (2.004, 2.004, 2.04), the expected new positions are (2.013, 1.947, 1.887).

The calculations of the EPR spectra of frozen metalloprotein solution must take into account the distribution of magnetic parameters due to strain effects in the sample. The **g – strain** tensor values for FeS cluster were found as "the best fit" parameters to the experimental EPR spectrum of magnetically isolated center. The inset below shows the simulations (*red*) of experimental "powder spectra" (*black*) at X - and Q – band. The parameters used for simulations were g = [2.023 1.89 1.775] and g-strain = [0.008(1), 0.008(1), 0.023(2)].

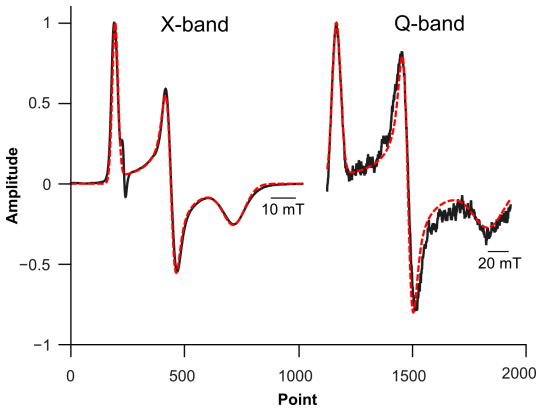

All numerical simulations of the EPR spectra were implemented in Matlab R.2008, using originally written procedures. The calculations of "powder spectra" for isolated paramagnetic center with S = $^1/_2$ implemented the simple algorithm by Hagen[6]. The simulations of the EPR spectrum of the coupled centers, including magnetic interactions required more complex approach. The matrix representation of the spin Hamiltonian (with specified orientation of the static magnetic field relative to the reference frame PAS of $\mathbf{g_1}$) was found using 4 basis vectors:

$$\left\{\left|m_{S_1}, m_{S_2}\right\rangle\right\} = \left\{\left|\frac{1}{2},\frac{1}{2}\right\rangle, \left|\frac{1}{2},-\frac{1}{2}\right\rangle, \left|-\frac{1}{2},\frac{1}{2}\right\rangle, \left|-\frac{1}{2},-\frac{1}{2}\right\rangle\right\}$$

After numerical diagonalization, eigenvalues and eigenvectors were obtained. Corresponding to the CW EPR detection mode (at constant microwave frequency), the resonance magnetic field position (B_{res}) was determined for each orientation, as well as transition probability appropriate for the perpendicular – mode – EPR (general formulas by Hagen were applied[6]). The resonance line as a function of magnetic field at constant frequency of applied microwaves was calculated according to Pilbrow scheme[7]. The g - strain broadening, defined originally in "g - values space", was consecutively transformed to the frequency, energy and magnetic field domain, using proper "re-normalization" formulas[8]. The final spectrum was a superposition of EPR signals originating from randomly oriented centers with respect to the applied magnetic field. The exact position of the middle line around g = 1.94 depended on the ratio between $|J_0|$ and $(g_2 - g_1)\beta B$, and the simulated spectra at both X – and Q – band were sensitive to the changes in J_0.

The experimental spectrum (W_{ex}) is a sum of the spectra of FeS clusters and the SQ_o-FeS coupled centers in identical proportions when measured at X – and Q – band. Therefore the simulated spectrum (W_{sim}), used for comparison with the experimental spectrum, was constructed as the combination:

$$W_{sim}^{X,Q} = k_1 W_{sim-FeS}^{X,Q} + k_2 W_{sim-\dim}^{X,Q}(J_o)$$

for which the contributions from the FeS center and the SQ_o-FeS coupled centers (k_1, k_2, respectively) and J_0 value were determined as the minimum of the following differences:

$$\left|\left(W_{\exp}^{Q} - W_{sim}^{Q}\right)\right|, \quad \left|\left(W_{\exp}^{X} - W_{sim}^{X}\right)\right|$$

This procedure allowed us to estimate $J_0 \approx$ 3500(500) MHz. $|J_0|$ of order 3500 MHz is strong enough to generate the triplet state of coupled SQ_o – FeS when measured at X – band, but not sufficient to assure domination of the exchange coupling over the separate, individual Zeeman interactions for each center. This is reflected as a shift of the middle line in the Q – band spectrum of the coupled SQ_o – FeS centers.

Figures

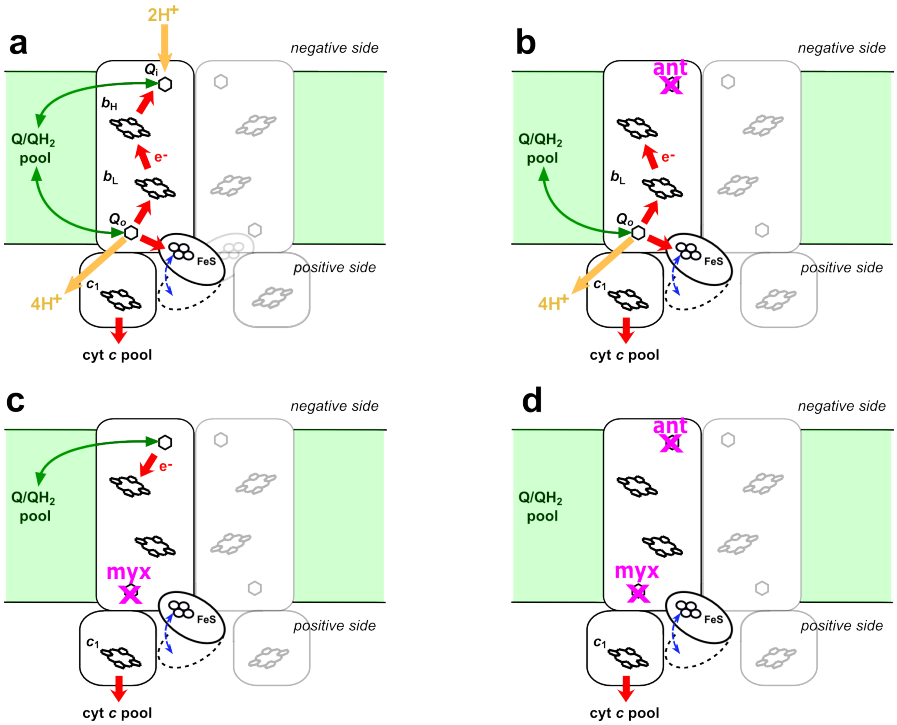

Figure S1. **Outline of catalytic cycle of cyt *bc*$_1$.** (**a**), Non-inhibited cyt bc_1 dimer catalyzes proton transfer across membrane coupled to electron transfer from membranous pool of ubiquinol (QH_2) to water-soluble pool of cyt *c*. At the Q_o site QH_2 undergoes two-electron oxidation in which one electron is transferred to the high – potential chain (c – chain), comprised of 2Fe-2S cluster (FeS) and heme c_1, while the second electron is transferred to the low – potential chain (b-chain) comprised of heme b_L, heme b_H and the Q_i site. FeS head domain naturally moves between the Q_o site and cyt c_1 (blue arrow) to support electron transfer in the c-chain (this movement is illustrated as two positions of round head domain housing FeS cluster). In the b-chain electron from heme b_L is transferred, through heme b_H to the Q_i site. Because full reduction of one molecule of Q at the Q_i site requires oxidation of two QH_2 molecules at the Q_o site (single electrons are delivered to the Q_i site sequentially with SQ_i intermediate state), releasing 4 protons to the *positive side* is coupled to the uptake of 2 protons from the *negative side* of the membrane (yellow arrows). (**b**), Antimycin inhibits the enzyme at the Q_i site. (**c**) Myxothiazol eliminates cyt bc_1 activity by blocking the Q_o site. Still however, QH_2 molecule can enter the Q_i site and reversibly reduce heme b_H forming well-known SQ_i radical which is easily detected by EPR. (**d**) Antimycin and myxothiazol together abolish any electron exchange between Q/QH_2 pool and cyt bc_1 cofactors. For simplicity, schemes **a**–**c** do not show possible electron transfer between the two hemes b_L in two monomers[9,10], and red arrows show only one direction of reversible electron transfer steps.

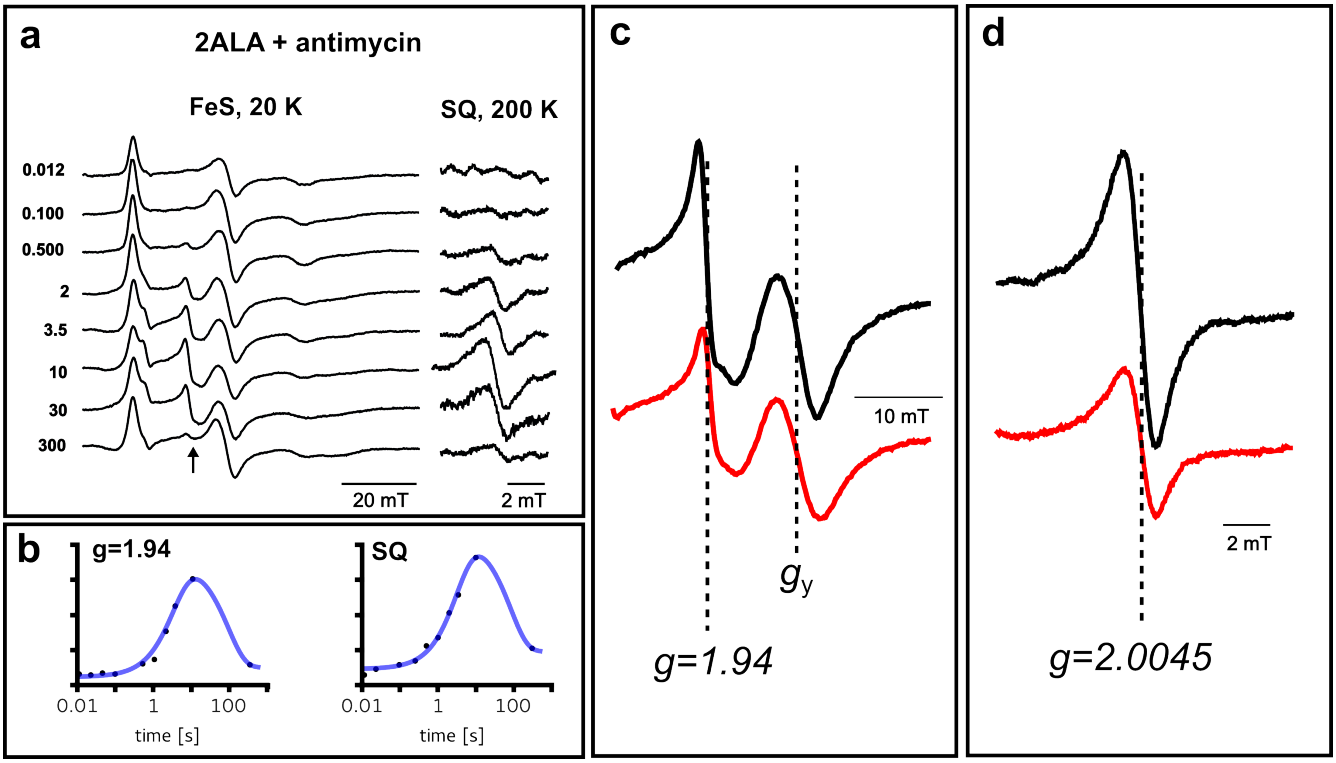

Figure S2. Monitoring changes in paramagnetic states of redox centers in +2Ala mutant of cyt bc_1 by X-band EPR during steady-state reduction of cyt *c* and oxidation of DBH_2. Samples were frozen at different time points after addition of DBH_2 to the mixture containing enzyme and cyt *c*. (**a**) In antimycin-inhibited +2Ala mutant the g = 1.94 (indicated by arrow) and g = 2.0045 signals appear similarly to WT cyt bc_1 (see Fig. 1B) despite higher level of initial reduction of FeS. (**b**) The time-course of these two signals are also similar as in WT cyt bc_1 (**c**) Comparison of maximum amplitudes of g = 1.94 signals obtained for the same quantities of +2Ala mutant (black*)* and WT (red) cyt bc_1. g_y indicates one of the transitions of the FeS cluster. (**d**) Comparison of maximum amplitudes of g = 2.0045 signals obtained for the same quantities of +2Ala mutant (black) and WT (red) cyt bc_1.

References

(1) Berry, E. A., Huang, L., Saechao, L. K., Pon, N. G., Valkova-Valchanova, M., and Daldal, F. (2004) X-Ray Structure of Rhodobacter Capsulatus Cytochrome bc_1: Comparison with its Mitochondrial and Chloroplast Counterparts. *Photosynth Res 81*, 251–275.

(2) Postila, P. A., Kaszuba, K., Sarewicz, M., Osyczka, A., Vattulainen, I., and Róg, T. (2013) Key role of water in proton transfer at the Q_o-site of the cytochrome bc_1 complex predicted by atomistic molecular dynamics simulations. *Biochim Biophys Acta 1827*, 761–768.

(3) Hoffmann, S. K., Hilczer, W., and Goslar, J. (1994) Weak long-distance superexchange interaction and its temperature variations in copper(II) compounds studied by single crystal EPR. *Appl Magn Reson 7*, 289–321.

(4) Moriya, T. (1960) Anisotropic Superexchange Interaction and Weak Ferromagnetism. *Phys Rev 120*, 91–98.

(5) Fournel, A., Gambarelli, S., Guigliarelli, B., More, C., Asso, M., Chouteau, G., Hille, R., and Bertrand, P. (1998) Magnetic interactions between a $[4Fe–4S]^{1+}$ cluster and a flavin mononucleotide radical in the enzyme trimethylamine dehydrogenase: A high-field electron paramagnetic resonance study. *J Chem Phys 109*, 10905–10913.

(6) Hagen, W. (2009) Biomolecular EPR Spectroscopy. CRC Press Taylor & Francis Group, Boca Raton.

(7) Pilbrow, J. K. (1988) New Insights and Trends in Transition Metal Ion Electron Paramagnetic Resonance. *Bull Magn Reson 10*, 32–64.

(8) Stevenson, R. C. (1984) Triplet state EPR spectra. *J Magn Reson 57*, 24–42.

(9) Swierczek, M., Cieluch, E., Sarewicz, M., Borek, A., Moser, C. C., Dutton, P. L., and Osyczka, A. (2010) An electronic bus bar lies in the core of cytochrome bc_1. *Science 329*, 451–454.

(10) Czapla, M., Borek, A., Sarewicz, M., and Osyczka, A. (2012) Enzymatic activities of isolated cytochrome bc_1-like complexes containing fused cytochrome *b* subunits with asymmetrically inactivated segments of electron transfer chains. *Biochemistry 51*, 829–835.